



# The role of ad-atoms in the coalescence of alkanethiol-passivated gold nanoparticles

C. Gutiérrez-Wing<sup>a</sup>, J.A. Olmos-Asar<sup>b</sup>, R. Esparza<sup>c,d</sup>, M.M. Mariscal<sup>b,\*</sup>, M.J. Yacamán<sup>d</sup>

<sup>a</sup> Instituto Nacional de Investigaciones Nucleares Ciencias Aplicadas-Tecnología de Materiales, Carr. México-Toluca S/N, La Marquesa Ocoyoacac, Edo. de México 52750, Mexico

<sup>b</sup> INFQ/CNICEt, Departamento de Matemática y Física, Facultad de Ciencias Químicas, Universidad Nacional de Córdoba, (XUA5000) Córdoba, Argentina

<sup>c</sup> Centro de Física Aplicada y Tecnología Avanzada, Universidad Nacional Autónoma de México, Boulevard Juriquilla 3001, Santiago de Querétaro, Qro., 76230, Mexico

<sup>d</sup> Department of Physics and Astronomy, University of Texas at San Antonio, One UTSA circle, 78249, San Antonio, TX, USA

## ARTICLE INFO

### Article history:

Received 17 September 2012

Received in revised form

21 December 2012

Accepted 25 December 2012

Available online 4 January 2013

### Keywords:

Monolayer-protected NPs

Coalescence

Sintering

Thiol-gold Cs-STEM

## ABSTRACT

In the present work we show how the role of ad-atoms and surface imperfections play a key role during the coalescence of thiol-passivated Au nanoparticles (NPs) below 4 nm in diameter. Using spherical aberration corrected scanning transmission electron microscopy (STEM) with ultra-high resolution and computer simulations we reveal the main structural and energetic changes throughout the diffusion/migration of surface atoms during coalescence of monolayer-protected NPs. The sintering process of nanoparticles with similar size (diameter) follows a neck-formation mechanism. However, in the case of thiol-protected Au NPs with different size (i.e. with dissimilar surface curvature) the Ostwald ripening mechanism has been detected with atomic resolution *in situ* STEM measurements for the first time. In particular we have observed how the larger particles grow in size at the expense of the smaller ones, until the latter completely disappear. The experimental findings have been supported with the aid of state-of-the-art computer simulations.

© 2012 Elsevier Ltd. All rights reserved.

## 1. Introduction

Metal nanoparticles supported on surfaces have traditionally attracted considerable attention due to their scientific and technological interest in electrocatalysis. Unfortunately, a thermodynamic-driven spontaneous process occurs, where large clusters grow at the expense of smaller – a phenomenon known as Ostwald ripening (OR). This process occurs because larger particles are more energetically favored than smaller ones. Therefore, finely dispersed nanoparticles have a tendency to aggregate. Therefore, it is of tremendous interest to understand the mechanism of (OR) or coarsening, in order to prevent it. As stated previously by Luque et al. [1], the observation of the OR mechanism is easier in the high-vacuum, where temperature, and hence the rates, can be varied over a wider range than in electrochemistry.

The synthesis of nanoscale materials inherently deals with the control of surface energy. When it is not properly controlled, it might lead to dimensional instabilities of the desired nanostructures through irreversible aggregation or coalescence processes [2,3]. These are among the most undesirable phenomena that can take place either during the synthesis of nanoparticles or after they are prepared, modifying their final properties. A widely

applied method to avoid these processes is stabilization of the nanostructures by surface passivation through the interaction of molecules of different nature with the surface of the nanoparticle [4]. Many approaches have been reported regarding the growth control and stabilization of nanomaterials, mainly of 0-D and 1-D nanostructures, and a key parameter to achieve this is based on the surface properties of materials and reactivity of exposed planes. Among the known synthesis methods, many have been developed within the frame of colloidal chemistry, where the stabilization of nanostructures can proceed by means of electrostatic repulsions – Faraday [5], Turkevich [6] – where counterions as citrate remain on the surface of suspended nanoparticles in polar solvents, or by surface reactions with surfactants or other organic molecules – Brust [7,8], Xia [9] where phosphines [10,11], amines [9,12], thiol molecules, etc., have a strong interaction with the atoms on the surface of the nanoparticles through the heteroatoms of these molecules. These kind of organic molecules, add functionality to the nanoparticle making it possible to tailor them for specific applications either in suspension or as a solid compound. A particularly successful method to produce small passivated gold nanoparticles proceeds through a two phase method in the presence of alkanethiol molecules, where size control is driven by a strong interaction of sulfur of these thiol molecules with the gold atoms on the surface of the nanostructure, obtaining a narrow particle size distribution. By other hand, it has been observed that these nanoparticles present mobility overmost substrates, as the

\* Corresponding author. Tel.: +54 351 5353853.

E-mail address: [marmariscal@fcq.unc.edu.ar](mailto:marmariscal@fcq.unc.edu.ar) (M.M. Mariscal).

amorphous carbon of TEM grids, and after some time, certain coalescence processes can be present, increasing the nanoparticle size range and their average diameter.

Closer analysis of these nanoparticles through HAADF-STEM has evidenced the presence of ad-atoms on their surface within the size range of 1–4 nm [13], reporting a bond energy of S–Au<sub>adatom</sub> of –2.93 eV, which is very close to that of Au–Au on particles, –3.14 eV on borders and –3.44 on Au(1 1 1) surfaces. This has been attributed as the origin of crystal structure distortions of the smallest capped nanoparticles, obtaining even amorphous nanostructures.

Further studies on the behavior of these nanoparticles under the low energy irradiation during their observation under the STEM mode are reported in this paper, as well as a thermodynamic study performed under classical simulations approaches, analyzing the role of these ad-atoms in the coalescence process of alkanethiol-passivated gold nanoparticles.

## 2. Experimental

### 2.1. Synthesis of gold nanoparticles

Based on the two-phase method reported by Brust et al. [9,10], gold nanoparticles passivated by 1-dodecanethiol were synthesized. Under constant stirring, 2 mL of a 0.1 M aqueous solution of hydrogen tetrachloroauratetrihydrate (HAuCl<sub>4</sub>·3H<sub>2</sub>O) are mixed at room temperature with a solution of 1.0 mmol of tetraoctylammonium bromide (N[C<sub>8</sub>H<sub>17</sub>]<sub>4</sub>Br) dissolved in 20 mL of toluene. After 1 h, 0.3 mL of 1-dodecanethiol (C<sub>12</sub>H<sub>25</sub>SH) and 6 mL of a 0.4 M aqueous solution of sodium borohydride (NaBH<sub>4</sub>) were added. The passivated nanoparticles were collected after 3 h and purified by precipitation in ethanol from the organic phase. All chemicals were used without any further purification.

### 2.2. Characterization

Alkanethiol-passivated nanoparticles were suspended in toluene. A drop of this suspension was deposited onto holey carbon copper grids. The samples were analyzed using spherical aberration (Cs) corrected scanning transmission electron microscopy (STEM) with a JEOL JEM-ARM200F microscope at 200 kV and a 80 picometer resolution, equipped with a Cs-corrector (CEOS GmbH) on the illumination system for the electron probe. The probe size used for acquiring the high-angle annular dark-field (HAADF) STEM images was 9C (23.2 pA) and the condenser lens (CL) aperture size was 40 μm. HAADF-STEM images were acquired with a camera length of 80 mm and the collection angle of 50–180 mrad was used, easily satisfying the requirement for the detector to eliminate contributions from unscattered or low-angle scattered. The electron probe correction was performed through the CESCOR software. The HAADF-STEM images were acquired using the DigiScanSTMPack system of the DigitalMicrograph™ software from Gatan.

## 3. Computations

Langevin dynamics (LD) calculations were performed to study the energetic stability during the growing of a large 1-butanethiol gold nanoparticle at the expenses of a smaller one. The semiempirical potential developed recently by Olmos-Asar and Mariscal [14] was used to represent the interatomic interaction of the complex S–Au interface (see Ref. [14] for further details). The second order approximation of the thigm binding (SMTB) theory was employed to model the Au–Au interaction with the same parameters as reported in Ref. [14], and the universal force field (UFF) was used to represent the inter and intra-molecular interactions of the organic molecules.

**Table 1**  
Size and separation distances of nanoparticles shown in Fig. 2.

| Nanoparticle | Size (nm) | Separation (nm)         | Process |
|--------------|-----------|-------------------------|---------|
| A            | 3.5       | A–B = 0.537             | 1       |
| B            | 3.7       |                         |         |
| C            | 3.0       | C–A = 0.807 C–B = 0.855 | 2       |
| D            | 2.6       | B–D = 0.581             | 3       |

For the LD simulations, a home-made code was used, where the Ermak algorithm was implemented to obtain the trajectories following the Langevin equations of motion, where the temperature is maintained at 200 K.

In our model, we placed initially two thiol-passivated gold nanoparticles of different size (Au<sub>147</sub> ≈ 1.5 nm and Au<sub>923</sub> ≈ 3.3 nm) at a short distance one from the other. Previously, the optimal coverage degree was determined using the same procedure as in Ref. [14]. Subsequently, Au or Au-SR units are detached from the smallest nanoparticle (keeping the coverage degree as stated in Ref. [14]) and added to the largest one (see a schematic representation in Fig. 4). Once this procedure has been concluded, the system evolves in order to reach equilibrium configurations (relax the structures). The routine is repeated until the smallest particle completely disappears.

## 4. Results and discussion

### 4.1. Experimental

Following the described procedure, gold nanoparticles passivated by 1-dodecanethiol were obtained as a brown solid. HAADF-STEM analysis was focused on nanoparticles smaller than 4 nm. During observation through this electron microscopy technique, where the electron radiation that reaches the samples is known to be less damaging to samples than in conventional TEM analysis, different features were analyzed. It was noted that nanoparticles had atoms on their surface with separation distances that did not agree with the known atomic distance of gold and did not form part of the crystalline core of the nanoparticle. In this sense, it has been reported (Ref. [13] and references therein) that due to the interaction of gold atoms with sulfur of thiol molecules, surface metallic atoms tend to be unstable with respect to the central metallic core creating distortions on the surface of the particle. The presence of these ad-atoms has been explained for small alkanethiol-protected nanoparticles of a few nanometers. As the particle size decreases, the S–Au bond has strength similar to that of the Au–Au bond as in the case of very small gold clusters. It has been reported that as the dimensions of nanoparticles within this size range become smaller, the distortion of the crystalline ordering is greater. In larger nanoparticles toward 4 nm, the core shape is maintained while the outer layer presents high distortions, allowing the identification of the so-called ad-atoms (Fig. 1).

Irradiation of the samples with the electron beam at 200 kV during STEM analysis seems to trigger the destabilization of ad-atoms in nanoparticles toward coalescence processes among 1-dodecanethiol passivated nanoparticles. Even when coalescence in this system has been extensively reported, we present here new insights on the first stages of coalescence not reported before under HRTEM observation modes.

Coalescence sequence was followed between different nanoparticles, observing different phenomena. The study was focused on the four nanoparticles presented in Fig. 2a. Separation between nanoparticles and their sizes are shown in Table 1.

Analysis of the observed phenomena was separated in three different processes.

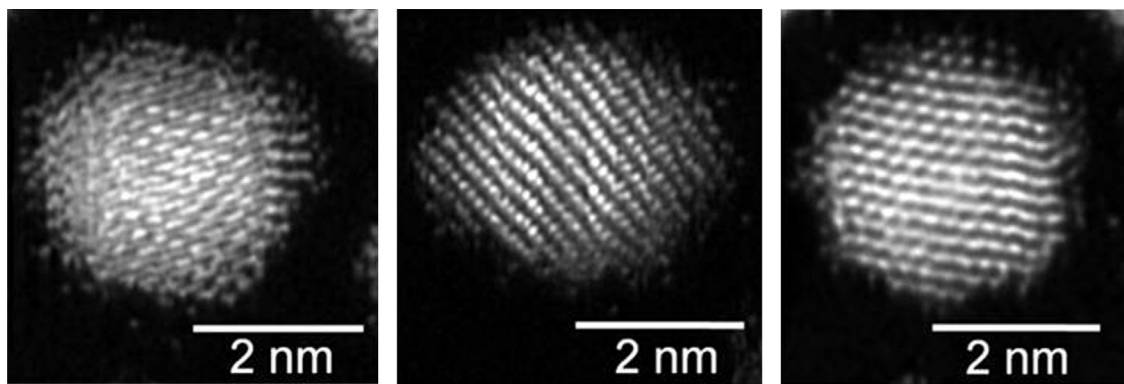


**Fig. 1.** Typical gold nanoparticles passivated by 1-dodecanethiol. Note the presence of ad-atoms on the surface of the nanoparticles.

#### 4.1.1. Process 1

In the first process, analysis of the phenomenon between A and B (initially with similar sizes, Fig. 2b) is presented. At the beginning, ad-atoms on the surface of particles A and B (Fig. 2c–d) form a bridge between both nanoparticles, even before an alignment of the crystalline planes could be noticed. This alignment occurs a few seconds after the formation of the bridge. Image on Fig. 2c shows a few ad-atoms between nanoparticles C–A and C–B as indicated by the arrow, which identifies the second process. Apparently, the migration of atoms between C and A–B stops at this point.

After this stage, sintering proceeds as it has been reported before (figure e–o), forming a neck between both nanoparticles A and B, until a new structure with a spherical tendency is formed. During this process, both nanoparticles continue changing in size and as particle A reduces gradually, particle B dominates by increasing its size. Also, atomic planes in both nanoparticles are reoriented in the same direction as can be seen in Fig. 2f.

Even when nanoparticles are passivated by 1-dodecanethiol, the energy supplied by the electron beam is enough to promote coalescence between nanoparticles by destabilization of ad-atoms. As observed from the results, a preferential coalescence was observed. The fact that the coalescence took place between nanoparticles A and B could be explained in terms of the potential energy, because it results energetically almost equivalent to the atoms to be on any of those particles with similar sizes (3.5 and 3.7 nm).

#### 4.1.2. Process 2

Since particle C is farther apart from A and B than the distance separating these two (see Table 1), it was more likely to begin the coalescence between these latter, where ad-atoms are closer and more attracted between them. In Fig. 2o, it can be seen that the new structure formed from the coalescence between A and B has reached and almost spherical shape which becomes more evident in Fig. 2p. At this stage where no more significant restructuration in the new particle A–B is observed, the sintering process between C and this new structure begins.

#### 4.1.3. Process 3

A particular phenomenon was given between particles D and B before and after the coalescence of A and B. As can be noticed in Fig. 2a, between these two particles D and B, few atoms are aligned as marked by the square, these seem to be ad-atoms aligned and deformation of both nanoparticles is not observed. After this stage, no more atoms in between could be detected, however, particle D deforms toward B (Fig. 2f–l). From Fig. 2m–o, particle D retracts again showing a FCC structure that deforms again (Fig. 2p) toward B, and this time a few atoms between them can be detected. After this stage, even when no coalescence neck or plane slip could be observed, particle D starts loosing ordering, crystallinity and size,

and eventually it is transformed into an randomly arranged group of atoms, until no more atoms of particle D could be observed.

Particle D was incorporated to particle B, probably through a diffusion mechanism, not following the neck-like formation between them. Instead, even when a deformation of the smaller nanoparticle toward particle B was noticed, it begins to lose crystalline ordering, and also fewer atoms are observed on the remaining cluster, as can be observed in Fig. 3. The group of atoms forming the cluster, with time seems to diffuse over to the surface of particle B (after coalescence and atom reordering between A–B finished).

A higher atomic disorder is observed in the smaller nanoparticle (D) which can be understood in terms of the larger surface-to-volume ratio. Evenmore, as stated in Ref. [13], the adsorption of thiol molecules on smaller Au nanoparticles produces a strong surface disorder, which finally makes the ad-atoms unstable. These surface atoms are influenced by the attraction potential of the large particle (B) diffusing toward it. However, a component of the van der Waals interaction of the alkyl chains with the substrate allows small particles to remain attached to the carbon surface until all atoms have migrated to the large particle. The observed phenomenon resemble the so-called surface-mediated Ostwald ripening mechanism where evaporation/diffusion of atoms from the smaller cluster toward the larger one occurs due to the difference on the chemical potential of both clusters.

#### 4.2. Computer simulations

Using the LD procedure described above, we have observed that the growing of the largest particle at the expenses of the smallest one is energetically favorable, as the energy of the system reduces significantly, once the process has finished. The selection of the atom/group of atoms to be transferred is due on the basis of the most stable coverage degree for the nanoparticle size, as explained before, and the coordination of the gold atoms: low coordinated atoms (which means, with less cohesive energy) have priority in the migration process.

Fig. 5 shows the computed potential energy per atom as a function of the number of gold atoms ( $N_{Au}$ ) transferred from the smallest particle to the largest one. As can be observed in the figure the overall process is energetically favorable. However, several local minima are detected indicating that the system could be trapped on them.

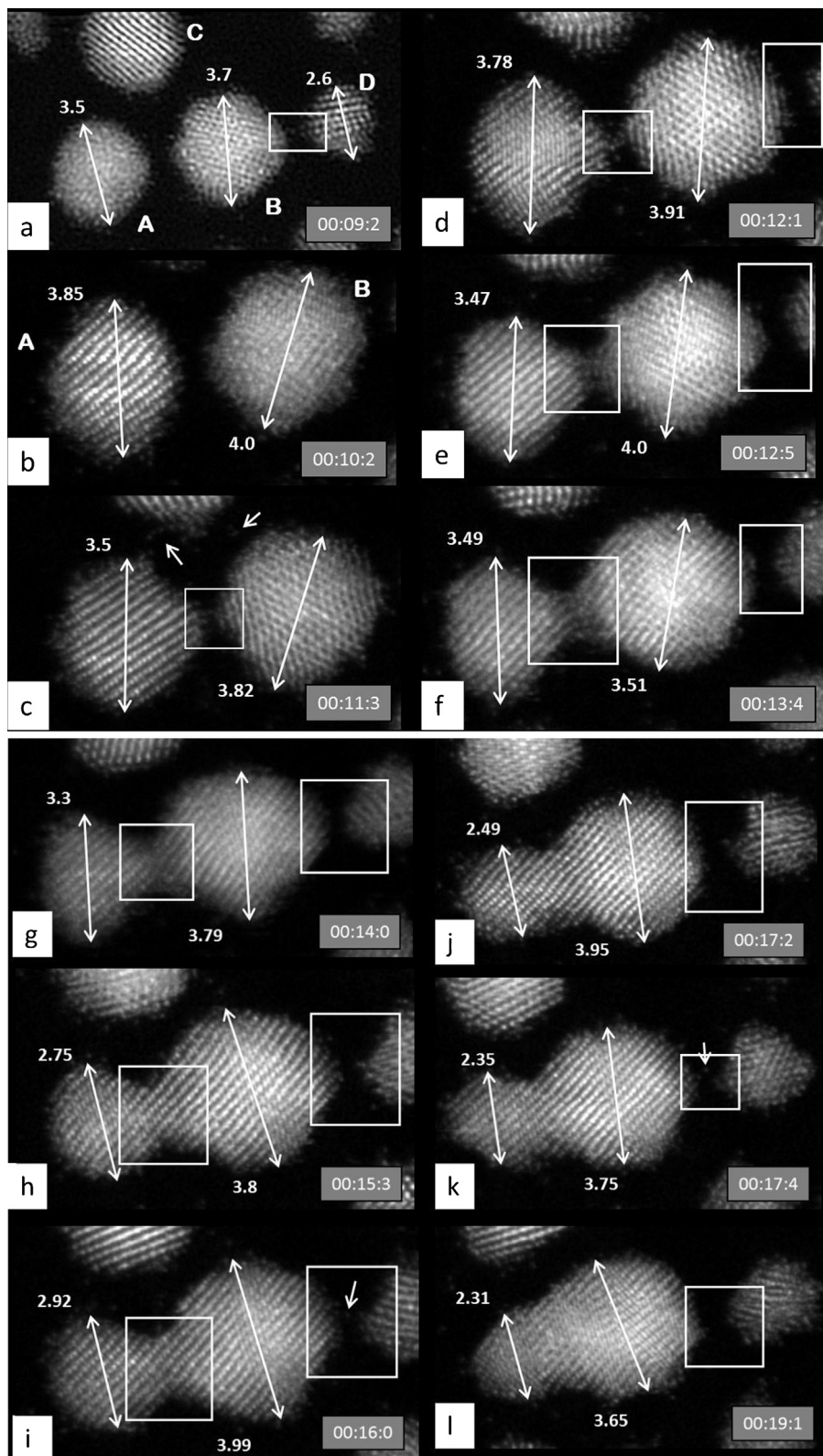
In this case no plane gliding is followed as reported previously for a conventional coalescence process through the Frank–Read mechanism [15], where the center of gravity of the nanoparticles changes as coalescence proceeds, until a new larger particle is formed as in the A–B coalescence process.

The fact that coalescence proceeds in nanoparticles that are covered by alkanethiol molecules could be attributed to a

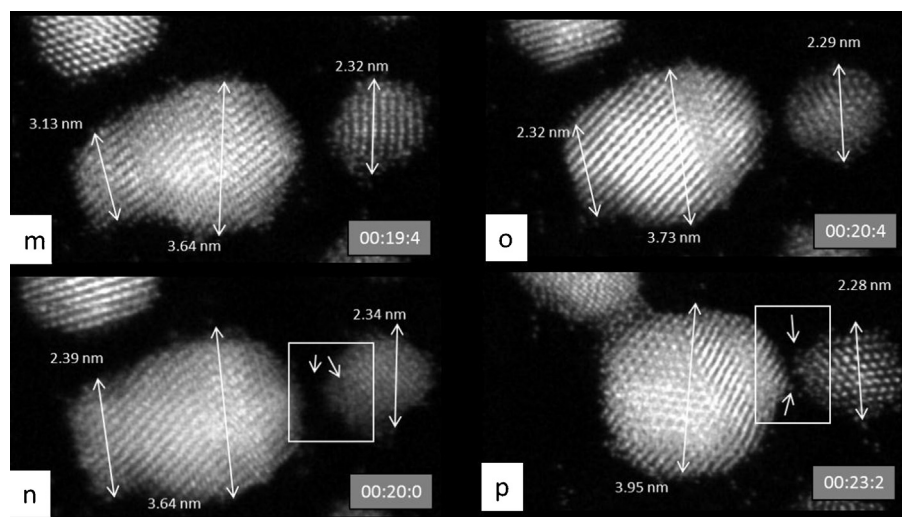
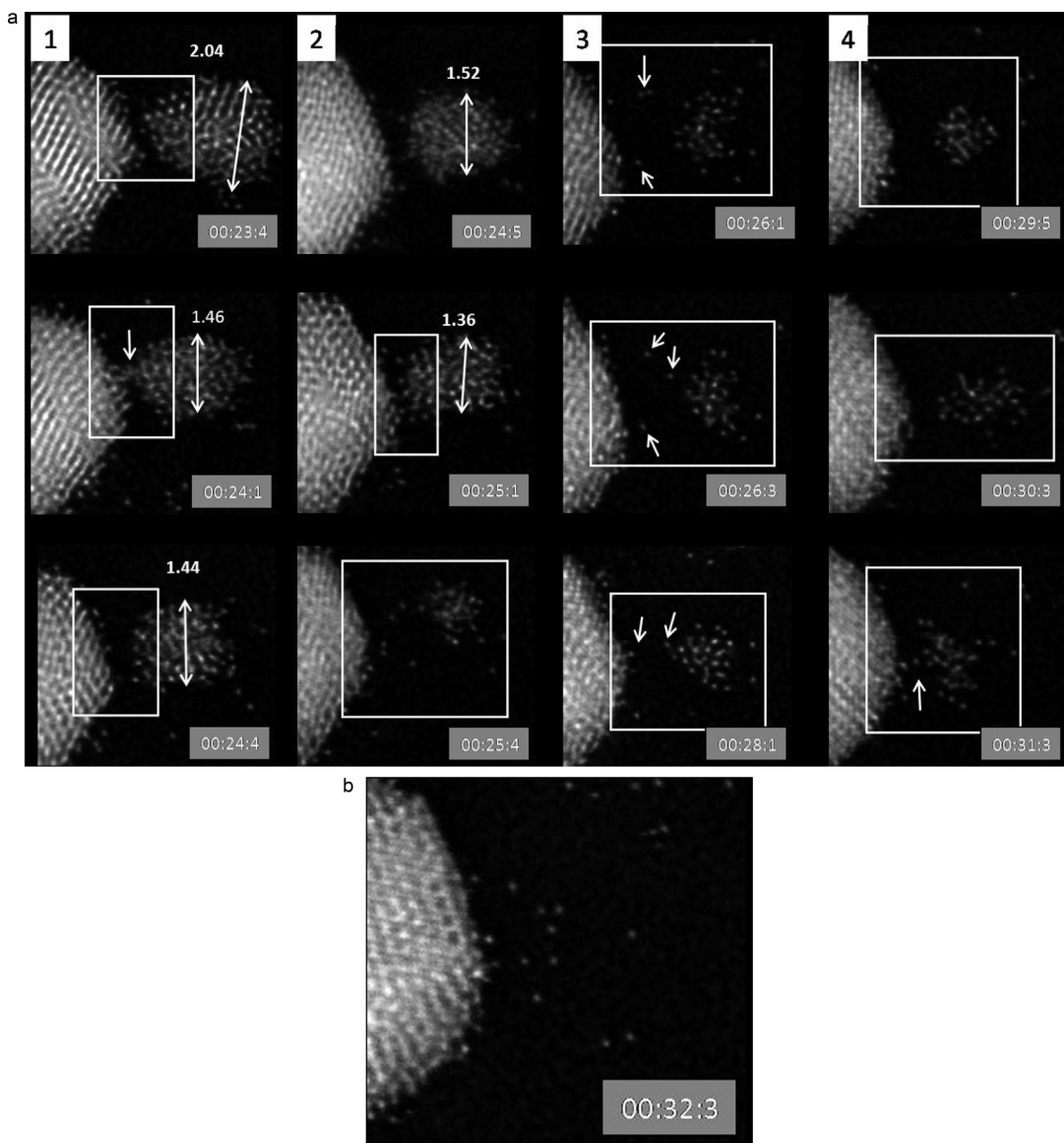
destabilization of the surface of the nanoparticles due to an initial migration of ad-atoms. Since these ad-atoms are reoriented between larger nanoparticles (A–B), where the interaction potential is also larger, atom migration from C to A and B remains

slower until the structure formed from coalescence between A and B is stabilized with a tendency to sphericity.

We have repeated the procedure for naked gold nanoparticles of the same sizes. In this case, only gold atoms were transferred



**Fig. 2.** Coalescence of nanoparticles with different sizes and distances between them (processes 1 and 2). Observe the presence of ad-atoms (c–d) between nanoparticles A, B, and C even before any restructuring becomes noticeable (e–p). Atoms between particles B and D are observed since the beginning of the process (a). Time of the process is indicated on the inset (h:m:s).

**Fig. 2.** (Continued).**Fig. 3.** Diffusion of atoms from particle D (process 3). Once the new structure formed by the coalescence of particles A–B–C (Fig. 2) stops showing restructuration, a modification in particle D becomes noticeable within a few seconds. Arrows indicate the diffusion of atoms from D to the new structure A–B–C presented in Fig. 2, until all atoms become part of one new structure. Time of the process is indicated in the inset (h:m:s).

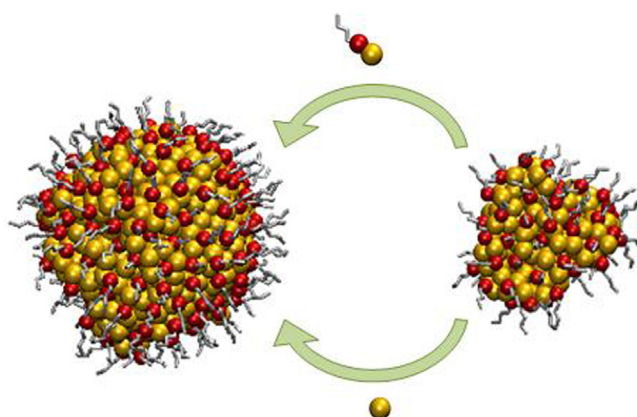


**Fig. 4.** Model system employed to study the energetic stability during coalescence of thiol-passivated Au nanoparticles. Au and RS/Au units are able to migrate from the smaller toward the larger particle.

from the small particle to the largest one in each stage of growing, and the system was relaxed. The graph of potential energy as a function of the number of transferred gold atoms is shown in Fig. 6. The red arrow points the final potential energy, which corresponds to the state in which only one nanoparticle remains, composed of  $923 + 147 = 1070$  gold atoms. The generation of a unique metal nanoparticle is energetically more stable than the existence of two separated particles, due to the reduction of the total surface. This is true even when the final structure is not symmetrical, and the starting ones correspond to structures defined by icosahedral magic numbers (lowest energy structures). Anyway, stabilization is less strong than in the case in which molecules are attached to the surfaces.

The coalescence of two unprotected gold nanoparticles of 923 and 147 gold atoms was also simulated. We found that this process is not activated, in contrast with the OR mechanisms reported before for Au NPs, and the energy corresponding to the final configuration is smaller than the initial one. The potential energy as a function of the simulation time (in unit of LD steps) is shown in Fig. 7. As observed, 0.007 eV per atom is gained due to the change in the surface-to-volume ratio. That is, the resulting nanoparticle after coalescence has an area smaller than the sum of the areas of the two isolated nanoparticles before coalescence.

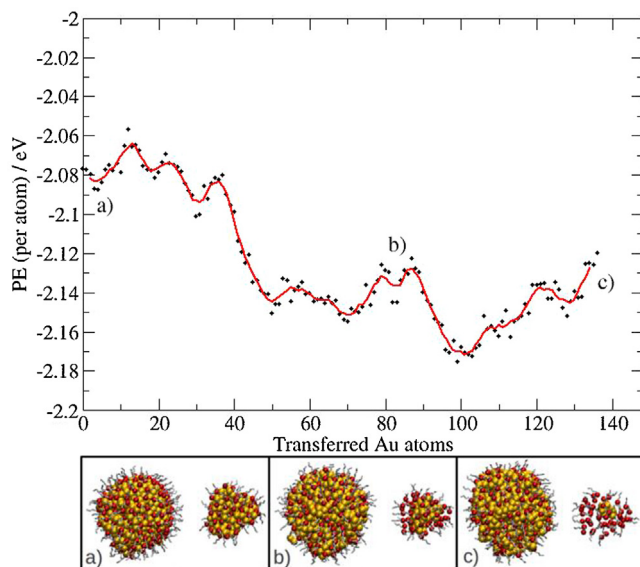


**Fig. 5.** Potential energy per atom as a function of the number of transferred Au atoms. Some selected configurations of the larger (left) and smaller (right) nanoparticles are shown.

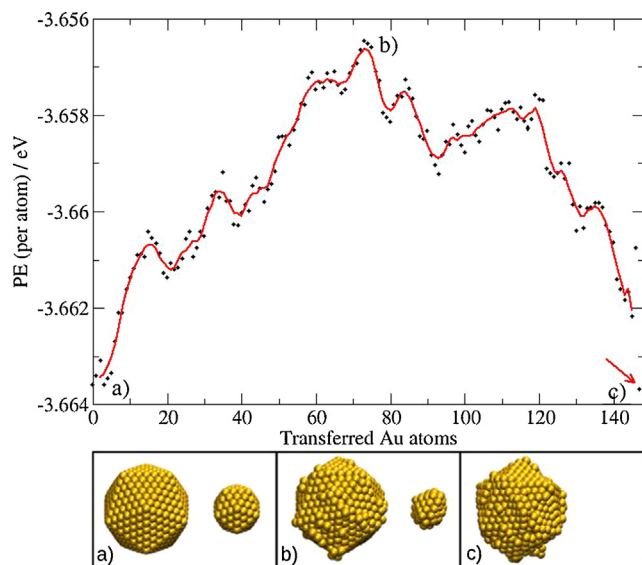


**Fig. 6.** Potential energy per atom as a function of the number of transferred Au atoms in absence of thiol molecules. Some selected configurations of the larger (left) and smaller (right) nanoparticles are shown. (For interpretation of the references to color in the text, the reader is referred to the web version of the article.)

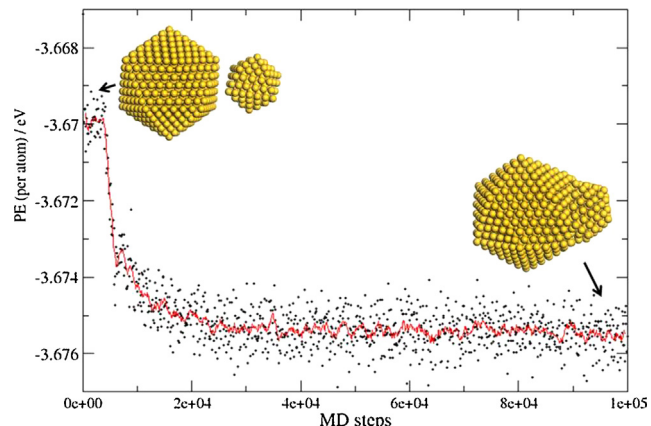


**Fig. 7.** Total potential energy as a function of the number of MD steps (time) during coalescence of ( $\text{Au}_{147} \approx 1.5 \text{ nm}$  and  $\text{Au}_{923} \approx 3.3 \text{ nm}$ ) in absence of thiol molecules. Inset: initial (before coalescence) and final configuration taken from the MD trajectories.

## 5. Conclusions

Following the Ostwald ripening (OR) model, atoms detach from small nanoparticles and move randomly over the substrate surface until they find another particle to join. It should be considered that small nanoparticles lose atoms at a higher rate as compared to larger clusters, because of the lower average coordination of atoms at the surface. As a result of this phenomenon, the larger particles grow in size at the expense of the smaller ones, until the latter completely disappear.

Experimental evidence shows that even when the surface of a gold nanoparticle has been passivated, in this case with 1-dodecanethiol, the formation of ad-atoms and the consequent distortion of the surface can lead to destabilization of the nanoparticles through an energetically driven process of migration of atoms between small nanoparticles. This destabilization eventually leads to the known coalescence process.

By means of computer simulations, we confirm that the OR mechanism between two thiol-protected gold nanoparticles mediated by ad-atoms or thiol-ad-atoms migration is energetically

favorable. The OR mechanism in unprotected gold nanoparticles is an activated process, while the coalescence of two unprotected gold NPs does not show any activation energy barrier to proceed.

In conclusion, in this work we were able to observe – *in real time* and *in situ* high resolution STEM – the diffusion of single atoms responsible for the surface mediated Ostwald-ripening mechanism. The energetic contributions of such mechanism were confirmed through computer simulations using a recently developed semiempirical potential for S–Au interfaces.

## Acknowledgements

The authors would like to acknowledge the NSF for support with grants DMR-1103730, “Alloys at the Nanoscale: The Case of Nanoparticles Second Phase and PREM: NSF PREM Grant # DMR 0934218; “Oxide and Metal Nanoparticles – The Interface Between Life Sciences and Physical Sciences”. MMM wish to acknowledge CONICET PIP 112-200801-000983 “Nanotechnology *in-silico*”, SECyT-UNC, PICT-Bicentenario 2010-123 for their financial support. JOA thanks CONICET for the fellowship. CGW wish to thank ININ CA-216 and CONACYT CB-169682 for the financial support.

## References

- [1] N.B. Luque, H. Ibach, K. Poetting, W. Schmickler, A simulation of two-dimensional Ostwald ripening on silver electrodes, *Electrochimica Acta* 55 (2010) 5411.
- [2] M.A. Asoro, D. Kovar, Y. Shao-Horn, L.F. Allard, P.J. Ferreira, Coalescence and sintering of Pt nanoparticles: *in situ* observation by aberration-corrected HAADF STEM, *Nanotechnology* 21 (2010) 025701.
- [3] A. Mayoral, S. Mejia-Rosales, M.M. Mariscal, E. Perez-Tijerina, M. José-Yacamán, The Co–Au interface in bimetallic nanoparticles: a high resolution STEM study, *Nanoscale* 2 (2010) 2647.
- [4] J.A. Olmos Asar, M.M. Mariscal, in: M.M. Mariscal, O.A. Oviedo, E.P.M. Leiva (Eds.), *Metal Clusters and Nanoalloys: From Modeling to Applications*, Springer, Berlin, 2012.
- [5] M. Faraday, Experimental relations of gold (and other metals) to light, *Philosophical Transactions of the Royal Society of London* (1857) 145.
- [6] J. Turkevich, P.C. Stevenson, J. Hiller, A study of the nucleation and growth processes in the synthesis of colloidal gold, *Discussions of the Faraday Society* 11 (1951) 55.
- [7] M. Brust, M. Walker, D. Bethell, D.J. Schiffrin, R.J. Whymann, Synthesis of thiol derivatised gold nanoparticles in a two phase liquid/liquid system, *Journal of the Chemical Society, Chemical Communication* (1994) 801.
- [8] C. Gutiérrez-Wing, P. Santiago, J.A. Ascencio, A. Camacho, M.J. Yacamán, Self-assembling of gold nanoparticles in one, two, and three dimensions, *Applied Physics A: Solids and Surfaces* 71 (2000) 237.
- [9] C. Xu, L. Sun, L.J. Kepley, R.M. Crooks, A.J. Ricco, Molecular interactions between organized, surface-confined monolayers and vapor phase probe molecules. 6. *In-situ* FTIR-external reflectance spectroscopy of monolayer adsorption and reaction chemistry, *Analytical Chemistry* 65 (1993) 2102.
- [10] P.M. Shem, R. Sardar, J.S. Shumaker-Parry, One-step synthesis of phosphine-stabilized gold nanoparticles using the mild reducing agent 9-BBN, *Langmuir* 25 (23) (2009) 13279.
- [11] J.M. Pettibone, J.W. Hudgens, Gold cluster formation with phosphine ligands: etching as a size-selective synthetic pathway for small clusters? *ACS Nano* 5 (4) (2011) 2989.
- [12] B.-K. Pong, J.-Y. Lee, B.L. Trout, First principles computational study for understanding the interactions between ssDNA and gold nanoparticles: adsorption of methylamine on gold nanoparticulate surfaces, *Langmuir* 21 (2005) 11599.
- [13] M.M. Mariscal, J.A. Olmos-Asar, C. Gutiérrez-Wing, A. Mayoral, M. José-Yacamán, On the atomic structure of thiol-protected gold nanoparticles: a combined experimental and theoretical study, *Physical Chemistry Chemical Physics* 12 (2010) 11785.
- [14] J.A. Olmos-Asar, A. Rapallo, M.M. Mariscal, Development of a semiempirical potential for simulations of thiol-gold interfaces. Application to thiol-protected gold nanoparticles, *Physical Chemistry Chemical Physics* 13 (2011) 6500.
- [15] M. José-Yacamán, C. Gutierrez-Wing, M. Miki, D.Q. Yang, K.N. Piyakis, E. Sacher, Surface diffusion and coalescence of mobile metal nanoparticles, *Journal of Physical Chemistry B* 109 (2005) 9703.